Hindawi
Advances in Materials Science and Engineering
Volume 2020, Article ID 3642356, 11 pages
https://doi.org/10.1155/2020/3642356

Research Article

Study on Damage Model and Damage Evolution Characteristics of Backfill with Prefabricated Fracture under Seepage-Stress Coupling

Jifeng Hou[1,2] **Zhongping Guo**[1] **Weizhen Liu**[1] **Hengze Yang**[1] **and WenWu Xie**[1]

[1]*College of Mining and Safety Engineering, Shandong University of Science and Technology, Shandong Qingdao 266590, China*
[2]*College of Coal Engineering, Shanxi Datong University, Shanxi Datong 037003, China*

Correspondence should be addressed to Zhongping Guo; gzp57046@sdust.edu.cn

Received 27 September 2019; Revised 25 December 2019; Accepted 27 January 2020; Published 9 March 2020

Guest Editor: Ferdi Cihangir

Aiming at the backfill with prefabricated fracture under seepage-stress coupling, the concepts of fracture macrodamage, loaded mesodamage, seepage mesodamage, and total damage of backfill were proposed. Based on the macroscopic statistical damage model, the coupling effect of seepage, stress, and initial fracture was considered comprehensively and the damage model of backfill with prefabricated fracture under seepage-stress coupling was established. The mechanical properties of backfill with prefabricated fracture under different seepage water pressures and confining pressures were tested and the rationality of the model was verified. The research shows that the mechanical properties of backfill with prefabricated fracture under the seepage-stress coupling are determined by the seepage water pressure, the load, the initial fracture, and the coupling effect. Fracture and seepage have significant effects on the damage of the backfill. When the seepage water pressure is low, the fracture damage dominates; however, when the seepage water pressure is high, the seepage damage dominates; the total damage under the coupling action is more serious than the single factor. The development laws of the total damage evolution curves under different seepage water pressures and confining pressures are basically the same, and they show the S-shaped distribution law with the increase of the axial strain. With the increase of confining pressure, the damage effect of fracture and seepage on the backfill is weakened, indicating that the confining pressure has a certain inhibitory effect on the damage evolution of the backfill. The research results can provide a theoretical basis for the study of the stability of backfill with geological defects such as joints and fractures in deep high-stress and high-seepage water pressure coal mines.

1. Introduction

Backfill coal mining technology is an effective method to improve the utilization of coal resources and control surface subsidence. It has been widely used in China and has become one of the main means of green coal mining [1–8]. The stability of the backfill is an important factor to prevent the instability of the goaf and the subsidence of the ground surface [9, 10]. Cemented coal gangue backfill is a common backfill method in coal mines [11–14]. However, in actual engineering, the influence of coal mining disturbance, blasting impact, and poor backfill effect can lead to a large number of fractures inside the backfill, which can easily reduce the strength of the backfill, and then it will cause the overall instability of the backfill working surface and the sinking of the surface [15]. For the intact backfill, the initial damage is considered to be zero and the initial mechanical properties of the backfill with prefabricated fracture are largely different from the nondestructive state. In addition, with the deep development of underground mining, high geostress and high seepage water pressure have become another important factor, affecting the stability of the backfill, and the two factors together affect the stability of the backfill [16–18]. Therefore, it is necessary to study the damage mechanical properties of backfill with prefabricated fracture under the coupling action of seepage and stress.

At present, many scholars at home and abroad have studied the fracture initiation, propagation law, and strength degradation characteristics of rock with fractures and the influence of seepage on the permeability of rock materials. Hadi et al. [19, 20] found that there are two main types of fractures in fractured pozzolanic Portland cement samples: wing fractures and secondary fractures; as the number of fractures increases, the ultimate breaking load of the specimens decreases. Heek et al. [21] found that there are two kinds of mechanical mechanisms for fracture propagation in fractured rock: one is tensile stress alone, and the other is tensile stress and shear stress through experimental research. Liu et al. [22] studied the nonlinear flow characteristics of fluids at the intersection of rock mass fractures by means of the indoor permeable test and the charge-coupled body (CCD) camera visualization technology. Liu et al. [23] established an analytical model of nonlinear seepage parameters (permeability coefficient k and nonlinear coefficient b) of fractured rock mass based on Forchheimer equation for the nonlinear characteristics of flow-pressure curve of high-water pressure test. Wang et al. [24] carried out permeability tests of limestone fractures with different roughness, analyzed the influence of coupling effect of stress and seepage erosion on the surface morphology of rough fractures, and studied the evolution law of seepage characteristics.

The above literatures mainly were focused on the fracture initiation, propagation, and permeability characteristics of fracture-bearing rocks. However, there are few studies on the damage evolution characteristics of backfill with prefabricated fracture under seepage-stress coupling. In view of this, based on the macroscopic statistical damage model, comprehensively considering the coupling effect of seepage, stress, and initial fracture, the damage evolution model of backfill with prefabricated fracture under seepage-stress coupling was established and the damage evolution characteristics of backfill with prefabricated fracture under the seepage-stress coupling were studied and verified by laboratory test results. The research results can provide a theoretical basis for the study of the stability of backfill with geological defects such as joints and fractures in deep high-stress and high-seepage water pressure mines.

2. Damage Model of Backfill with Prefabricated Fracture under Seepage-Stress Coupling

2.1. Seepage Mesodamage of Backfill. Backfill is a kind of multiphase composite material with coal gangue, fly ash, and cement as cementitious materials, which has a lot of pores and fractures. Under the action of the seepage water pressure, the pores and fractures are expanded and connected, and the macroscopic performance is the deterioration of the mechanical properties of the backfill. The damage evolution law of microscopic and mesoscopic defects of the backfill under seepage conditions is very complicated. Since the damage degree of the backfill can be reflected by its external macroscopic mechanical properties, the macroscopic phenomenological damage mechanics method can be used to study the mesoscopic damage of the backfill under seepage conditions. According to the theory of damage mechanics, the seepage damage of the backfill is characterized by the change of mechanical parameters such as elastic modulus, and the damage variable of the seepage is defined as follows:

$$D_p = 1 - \frac{E_p}{E_0}, \tag{1}$$

where E_0 is elastic modulus of intact backfill; E_p is elastic modulus of intact backfill considering seepage.

2.2. Loaded Mesodamage of Backfill. The backfill is composed of a large number of microunits and the distribution of the mechanical properties of each microunit is random. The damage degree of the backfill is related to the defects contained in each microunit, and these defects directly affect the strength of the microunit. Therefore, there is the following relationship between the loaded damage variable D_s and the statistical distribution density function $\varphi(\varepsilon)$ of the microunit damage:

$$\varphi(\varepsilon) = \frac{\mathrm{d}D_s}{\mathrm{d}\varepsilon}, \tag{2}$$

where $\varphi(\varepsilon)$ is the measurement of the microunit damage rate of backfill during the loading process and the damage accumulation of microunit leads to the deterioration of the macroscopic performance of backfill. Assume that the microunit strength of backfill obeys the Weibull statistical distribution, the loaded damage variable D_s can be expressed as follows:

$$D_s = \int_0^{\varepsilon} \varphi(x)\mathrm{d}x = 1 - \exp\left[-\left(\frac{\varepsilon^*}{a}\right)^m\right], \tag{3}$$

where a, m are the distribution parameters, and ε^* is the microunit strain.

According to the strain equivalence principle proposed by Lemaitre [25], the constitutive relation of the damaged material is as follows:

$$\sigma = (1 - D_s)E_0\varepsilon. \tag{4}$$

From (2) and (3), it can be deduced that the loaded damage constitutive model of the backfill under pseudo-triaxial conditions is as follows:

$$\left.\begin{aligned} \sigma_1 &= E_0\varepsilon_1 \exp\left[-\left(\frac{\varepsilon^*}{a}\right)^m\right] + 2\mu\sigma_3 \\ (1-\mu)\sigma_3 &= E_0\varepsilon_3 \exp\left[-\left(\frac{\varepsilon^*}{a}\right)^m\right] + \mu\sigma_1 \end{aligned}\right\}. \tag{5}$$

Assume that the backfill obeys the Misses yield criterion and the Hooker theorem, the strain expression in equation (5) can be obtained as follows:

$$\left.\begin{aligned} \varepsilon_1^* &= \varepsilon_1 - \frac{(1-2\mu)\sigma_3}{E_0} \\ \varepsilon_3^* &= -\frac{\varepsilon_3}{\mu} + \frac{(1-2\mu)\sigma_3}{\mu E_0} \end{aligned}\right\}. \tag{6}$$

During the deformation and failure of the backfill, the stress-strain relationship at the peak point should satisfy the following geometric conditions: (1) When $\varepsilon_1 = \varepsilon_f$, $\sigma_1 = \sigma_f$

(2) When $\varepsilon_1 = \varepsilon_f$, $\partial\sigma_1/\partial\varepsilon_1 = 0$, where ε_f and σ_f are the strain and stress values at the extreme points of the stress-strain curve of the backfill, respectively.

According to the geometric conditions (1) and (2), the following can be derived from equations (5) and (6):

$$\left.\begin{aligned} a &= \left[\frac{\varepsilon_f - (1-2\mu)\sigma_3}{E_0}\right]\left[\frac{m\varepsilon_f}{\varepsilon_f - (1-2\mu)\sigma_3/E_0}\right]^{1/m} \\ m &= \frac{\varepsilon_f - (1-2\mu)\sigma_3/E_0}{\varepsilon_f \ln E_0\varepsilon_f/\sigma_f - 2\mu\sigma_3} \end{aligned}\right\}. \tag{7}$$

From equations (3) and (7), the loaded damage variable of backfill is as follows:

$$D_s = 1 - \exp\left\{\left[\frac{\varepsilon_1 - (1-2\mu)\sigma_3/E_0}{\varepsilon_f - (1-2\mu)\sigma_3/E_0}\right]^m \ln\frac{\sigma_f - 2\mu\sigma_3}{E_0\sigma_f}\right\}. \tag{8}$$

2.3. Mesodamage of Backfill under Seepage-Stress Coupling. According to the strain equivalence principle proposed by Lemaitre, the strain caused by the full stress σ acting on the damaged material is equivalent to the strain caused by the effective stress $\sigma\prime$ acting on the nondestructive material. Therefore, the constitutive relation of the damaged material can be derived from the constitutive equation of the nondestructive material. As long as the nominal stress is replaced by the effective stress, the internal damage constitutive relation of the backfill is as follows:

$$\sigma = E_0(1 - D_s)\varepsilon, \tag{9}$$

where E_0 is elastic modulus of intact backfill; D_s is loaded damage variable of intact backfill.

According to the generalized strain equivalence principle proposed by Zhang et al. [26, 27], the seepage damage is regarded as the first damage state, and the loaded damage state after seepage damage is regarded as the second damage state. The internal damage constitutive relationship of the backfill is as follows:

$$\sigma = E_p(1 - D_s)\varepsilon. \tag{10}$$

The stress-strain constitutive relation expressed by the seepage and the loaded damage variable can be obtained from equations (1) and (10) as follows:

$$\sigma = E_0(1 - D_m)\varepsilon, \tag{11}$$

where

$$D_m = D_s + D_p - D_s D_p, \tag{12}$$

D_m is the seepage-load coupling damage of the backfill, and $D_s D_p$ is the coupling term of the two kinds of damage.

Formula (12) shows that the damage of backfill is aggravated by the interaction of seepage and stress, but the total damage is not a simple superposition of seepage damage and loaded damage. The "–" sign before the coupling term indicates that the coupling effect of two stages of mesodamage reduces the total damage. According to the analysis, during the seepage process, the microdefects in the backfill are enhanced and the relative density is increased. Therefore, under the action of the load, the slip and displacement between the internal particles are hindered. During the loading process, the internal microdefects are closed and compacted, and the mesodefects are improved to alleviate the seepage damage.

From equations (1), (3), and (12), the damage evolution equation of the backfill under the action of seepage and load is as follows:

$$D_m = 1 - \frac{E_p}{E_0}\exp\left[-\left(\frac{\varepsilon^*}{a}\right)^m\right]. \tag{13}$$

2.4. Total Damage of Backfill with Prefabricated Fracture under Seepage-Stress Coupling. According to the theory of damage mechanics, the definition of damage variable is the premise and basis for the establishment of damage model. Therefore, the following is the first to discuss the damage variables of the backfill with prefabricated fracture under the seepage conditions, considering macroscopic and microscopic defects. The damage coupling of macroscopic and mesoscopic defects is concentrated as the coupling of damage variables.

In calculating the coupling of the damage variable of backfill with prefabricated fracture, the following basic assumptions are used: (1) Macroscopic damage and mesoscopic damage are visually and invisibly divided by human eyes and macroscopic and mesoscopic damage are considered to be isotropic damage. (2) The initial damage caused by the fracture to the backfill is defined as macroscopic damage D_1 and the damage caused by the seepage or the load is defined as mesoscopic damage D_2 and the coupling damage of seepage and load is D_{12}. (3) Coupling is based on the strain equivalent principle proposed by Lemaitre [25] and the two types of damage cannot be simply superposed.

As shown in Figure 1, it is assumed that Figures 1(a)–1(d), respectively, represent the backfill containing macroscopic and mesoscopic defects, the backfill only containing macroscopic defects, the backfill only containing mesoscopic defects, and the intact backfill [28]. The corresponding elastic moduli are, respectively, E_{12}, E_1, E_2, and E_0, and the corresponding strains under the action of external force are, respectively, ε_{12}, ε_1, ε_2, and ε_0. Based on the Lemaitre strain equivalence principle, then there is

$$\varepsilon_{12} = \varepsilon_1 + \varepsilon_2 - \varepsilon_0, \tag{14}$$

$$\frac{\sigma}{E_{12}} = \frac{\sigma}{E_1} + \frac{\sigma}{E_2} - \frac{\sigma}{E_0}. \tag{15}$$

From Lemaitre's hypothesis, we can see that

$$\begin{cases} E_{12} = E_0(1 - D_{12}), \\ E_1 = E_0(1 - D_1), \\ E_2 = E_0(1 - D_2). \end{cases} \tag{16}$$

Substituting Formula (16) into Formula (15), we can get the following formula:

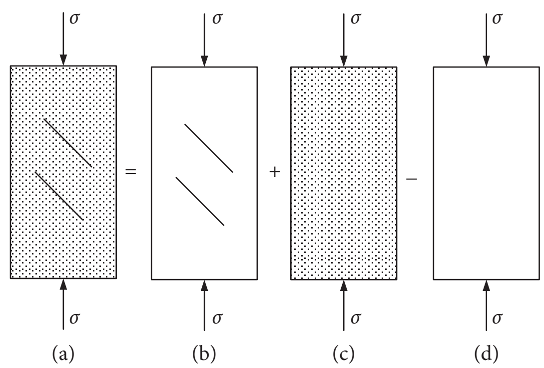

Figure 1: Schematic diagram of calculated equivalence strain.

$$D_{12} = 1 - \frac{(1 - D_1)(1 - D_2)}{1 - D_1 D_2}. \quad (17)$$

The initial damage state of the intact backfill is taken as the reference damage state, the damage caused by the prefabricated fracture is regarded as the macroscopic damage D_j, and the damage caused by the seepage and load coupling is regarded as the mesoscopic damage D_m. The total damage of the backfill with prefabricated fracture caused by the seepage-load coupling is regarded as the total damage D, then equation (17) is rewritten as follows:

$$D = 1 - \frac{\left(1 - D_j\right)(1 - D_m)}{1 - D_j D_m}, \quad (18)$$

where

$$D_j = 1 - \frac{E_j}{E_0}, \quad (19)$$

E_j is the elastic modulus of the backfill with prefabricated fracture.

Equations (13), (18), and (19) constitute a complete damage evolution model of backfill with prefabricated fracture, which takes into account the effects of seepage-stress coupling effects. The formula reflects the nonlinear characteristics of the interaction of seepage, load, and prefabricated fracture on the damage propagation of backfill. When the backfill is only affected by fracture, that is, $D_m = 0$, there is $D = D_j$; when the backfill does not contain macrodefects such as fractures, that is, $D_j = 0$, there is $D = D_m$.

According to the damage mechanics theory, the damage constitutive relation of the backfill with prefabricated fracture under the triaxial condition can be further deduced from formula (18):

$$\begin{cases} \sigma_1 = E_0 (1 - D)\varepsilon_1 + 2\mu_{jp}\sigma_3, \\ \left(1 - \mu_{jp}\right)\sigma_3 = E_0 (1 - D)\varepsilon_3 + \mu_{jp}\sigma_1, \end{cases} \quad (20)$$

where μ_{jp} is Poisson ratio of the backfill with prefabricated fracture considering seepage.

Formulas (13), (18)–(20) constitute a complete damage constitutive equation of backfill with prefabricated fracture considering seepage-stress coupling effect.

From the above deductions, it can be seen that the stress at any point of backfill with prefabricated fracture under seepage-stress coupling is related to the fracture, seepage water pressure, ultimate strength, peak strain, and strain at that point. The distribution parameter m of backfill characterizes the brittleness of backfill; that is, the smaller the value of m, the more the plastic failure of backfill tends to be. The macroscopic strength of backfill is characterized by a.

3. Laboratory Experiments

3.1. Experimental Equipment. In order to verify the rationality and reliability of the above damage evolution model, the author performed three-axis compression tests under the seepage-stress coupling on the MTS815 rock mechanics test machine, as shown in Figure 2.

The system mainly tests the mechanical properties and seepage characteristics of high-strength and high-performance solid materials under complex stress conditions. The main features of the system are as follows: ① It can realize automatic data collection and processing by full computer control. ② Three independent servo systems are equipped, including axial pressure (maximum axial load is 280000 kN), confining pressure (maximum confining pressure is 80 MPa), and pore water pressure (maximum pore pressure is 80 MPa). ③ The servo response is fast (290 Hz) and the test accuracy is high. ④ The extensometer can work in high temperature and high pressure oil and can accurately measure the stress and strain of rock. ⑤ The test can be carried out with arbitrary loading waveform and rate. ⑥ The closed-loop heating system can provide a uniform temperature field and the maximum temperature is 200°C. The specimen size is a cylinder of ϕ50 mm × 100 mm and ϕ100 mm × 200 mm.

3.2. Materials Characteristics. The raw materials of the backfill are made up of coal gangue, fly ash, cement, and water according to a certain ratio. Coal gangue was taken from the gangue mountain of Daizhuang Coal Mine for secondary crushing, with the particle size between 0.1 and 15 mm. The fly ash was taken from the class II fly ash of Qingdao Power Plant. The cement was 32.5 ordinary Portland cement produced by Shandong Shanshui Cement Group Limited. The main chemical components of raw materials are shown in Table 1.

According to the engineering requirement of backfill coal mining, the State Key Laboratory of Mine Disaster Prevention and Control, which the author works in, has carried out a lot of tests and determined the mix proportion of backfill specimen, as shown in Table 2.

The uniformly stirred slurry was poured into a mold, and a fracture was prefabricated by a thin iron piece, the angle of the fracture is 45°, the length of the fracture is 20 mm, and the width of the fracture is 2.0 mm. According to the International Rock Mechanics Society (ISRM) test procedure, the cylinder specimens with a diameter of ϕ50 mm × 100 mm were made. After 1 day of maintenance, the mold was released and placed in a standard curing box

(a) (b)

Figure 2: The test apparatus. (a) MTS815 rock mechanics test system. (b) Test specimen installation details.

Table 1: Chemical composition of the main raw materials of backfill specimen.

Major element	Coal gangue (%)	Cement (%)	Fly ash (%)
SiO_2	56.1	22.95	52.35
Al_2O_3	18.6	5.32	32.60
Fe_2O_3	4.6	3.90	2.51
CaO	2.34	62.58	8.13
MgO	1.31	2.06	0.95
SO_3	0.12	2.33	0.51
LOI	10.23	2.58	11.62

Table 2: Mix proportion of backfill specimen.

Raw materials	Coal gangue (wt%)	Fly ash (wt%)	Cement (wt%)	Concentration (wt%)
Proportion	55	36	9	74

(relative humidity 95%, temperature 20°C) for 28 days. Before the test, each side of the specimen is ground flat with sandpaper, and the processing accuracy meets the rock test standard.

3.3. Experimental Method. Experimental steps: (a) Seal and wrap the specimen with heat shrinkable tube, then install it on the base of the test machine after installing axial and circumferential extensometers, as shown in Figure 2(b). (b) Control the hydraulic pump to apply confining pressure σ_3 to a predetermined value and keep it unchanged. (c) Apply seepage water pressure p_1 and p_2 ($\sigma_3 > p_1 \geq p_2 = 0$ MPa), respectively, on the upper and lower ends of the specimen, so as to form a stable seepage pressure difference at both ends of the specimen. (d) Adopt displacement loading method; the loading rate is 0.02 mm/min and the loading is continued until the specimen is broken. During the loading process, the stress-strain curve of the specimen is automatically recorded by computer. The stress mode of backfill specimen is shown in Figure 3.

Considering the feasibility of testing instruments and the rationality of pressure setting, the seepage water pressure at the inlet end of the specimen was set to 0 MPa, 0.3 MPa, 0.6 MPa, 0.9 MPa, and 1.2 MPa, and the outlet end of the specimen was connected to the atmosphere and the confining pressure was set to 0.5 MPa, 1.0 MPa, 1.5 MPa, and 2.0 MPa. The specific experimental scheme is shown in Table 3.

3.4. Model Verification. In order to verify the correctness and rationality of the damage constitutive model established in this paper, the stress-strain curves are drawn by the constitutive model and the experimental data and compared with the experimental curves of backfill with prefabricated fracture under different seepage water pressures (as shown in Figure 4).

It can be seen from Figure 4 that the theoretical calculation curves before peak strain are highly consistent with the experimental curves; the stress-strain curves are approximately linear; the post-peak curves are poorly consistent, but the basic trend is the same. Generally speaking, the damage constitutive model of the backfill with prefabricated fracture established in this paper is in good agreement with the experimental curves in both curve law and numerical value and can better reflect the stress-strain relationship of the backfill with prefabricated fracture specimen under seepage-stress coupling action. It can be used to analyze the damage evolution characteristics of

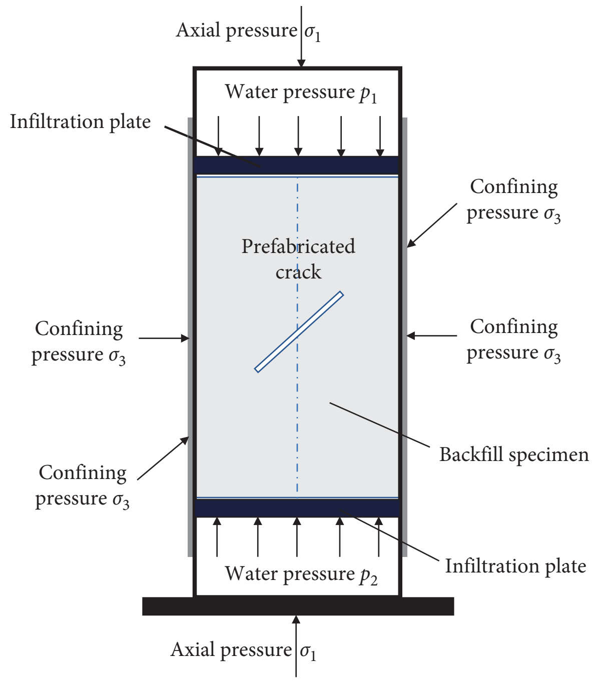

FIGURE 3: Loading diagram of backfill specimen.

TABLE 3: Experiment scheme.

Test number	Intact backfill specimens		Backfill specimens with prefabricated fracture		Remarks
	Seepage water pressure (MPa)	Initial confining pressure (MPa)	Seepage water pressure (MPa)	Initial confining pressure (MPa)	
1	0	1.5	0	1.5	Samples are saturated
2	0.3	1.5	0.3	1.5	
3	0.6	1.5	0.6	1.5	
4	0.9	1.5	0.9	1.5	
5	1.2	1.5	1.2	1.5	
6	0.3	0.5	0.3	0.5	
7	0.3	1.0	0.3	1.0	
8	0.3	1.5	0.3	1.5	
9	0.3	2.0	0.3	2.0	

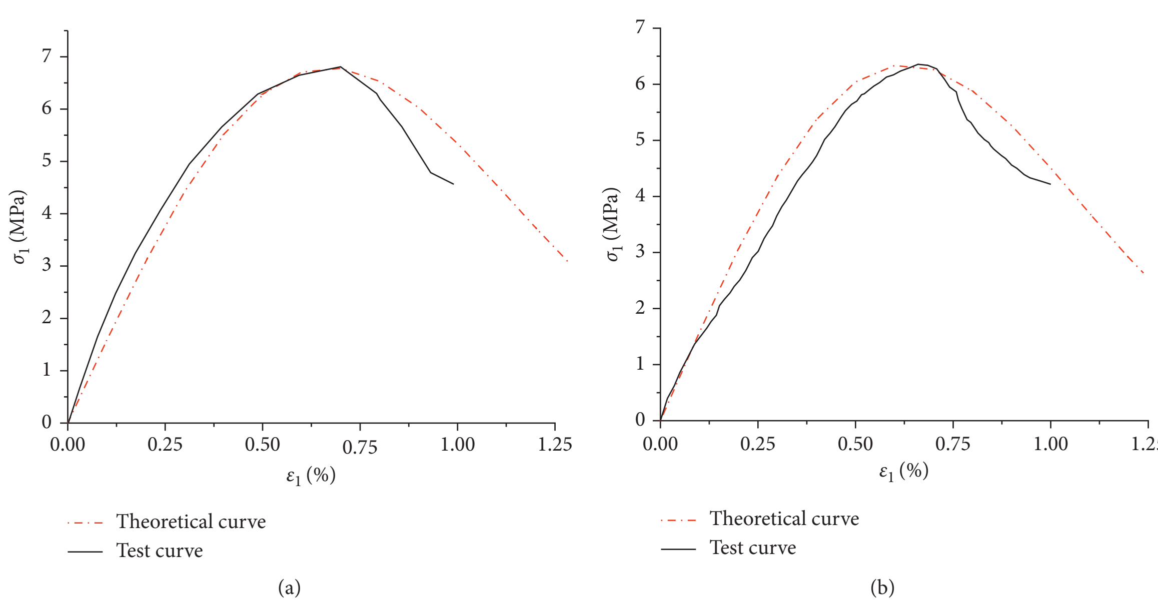

FIGURE 4: Continued.

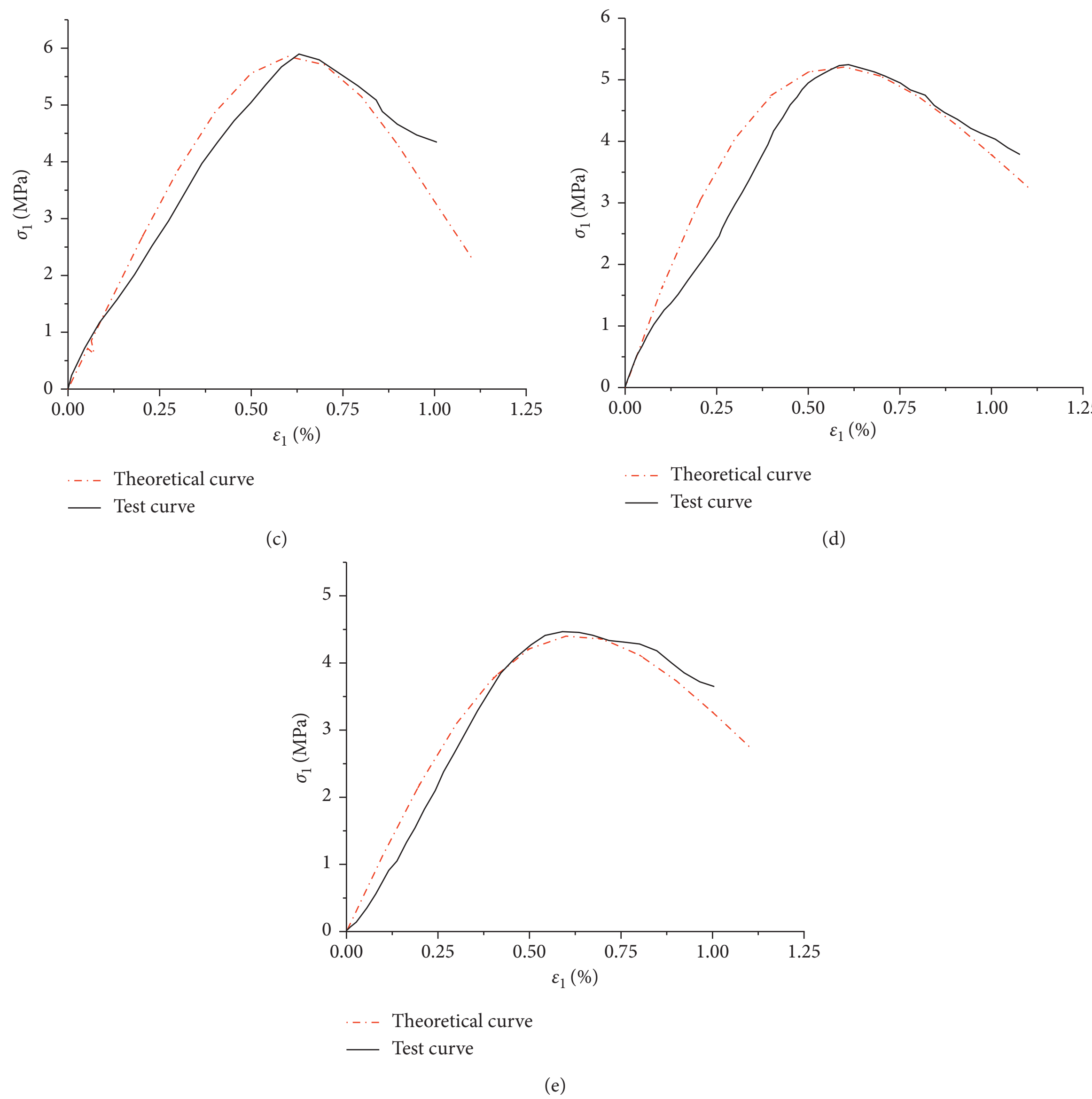

FIGURE 4: Calculated values of damage evolution model contrast with experimental values. (a) $p = 0$ MPa. (b) $p = 0.3$ MPa. (c) $p = 0.6$ MPa. (d) $p = 0.9$ MPa. (e) $p = 1.2$ MPa.

backfill with prefabricated fracture under seepage-stress coupling.

4. Damage Evolution Characteristics Analysis

4.1. Influence of Seepage on Backfill Damage. According to the mechanical parameters of the backfill under different seepage water pressures and formula (18), the intrinsic relationship between the seepage damage and the seepage water pressure can be obtained, as shown in Figure 5.

It can be seen from Figure 5 that there is seepage damage inside the backfill under the action of seepage, the seepage damage of the backfill increases with the increase of the seepage water pressure, especially in the presence of fractures, and the degree of damage is significantly different. Initial fracture damage D_j, seepage damage D_p, and seepage-fracture coupling damage D_{jp} were 0.16, 0.05–0.40, and 0.25–0.53, respectively.

It can be seen that fracture and seepage have a significant influence on the strength of backfill. Fracture damage dominates at low seepage water pressures, seepage damage dominates at high seepage water pressures, and total damage under the coupling action is more serious than that under single factor. Therefore, in the deep high-stress, high-permeability water-pressure mines, fractures in the backfill should be avoided as much as possible due to factors such as mining disturbance, blasting impact, or poor filling effect, so as to avoid the coupling effect to accelerate the damage development of the backfill.

Figure 6 shows the damage evolution curves of the backfill under different seepage water pressures when the confining pressure is 1.5 MPa. It can be seen in Figure 6.

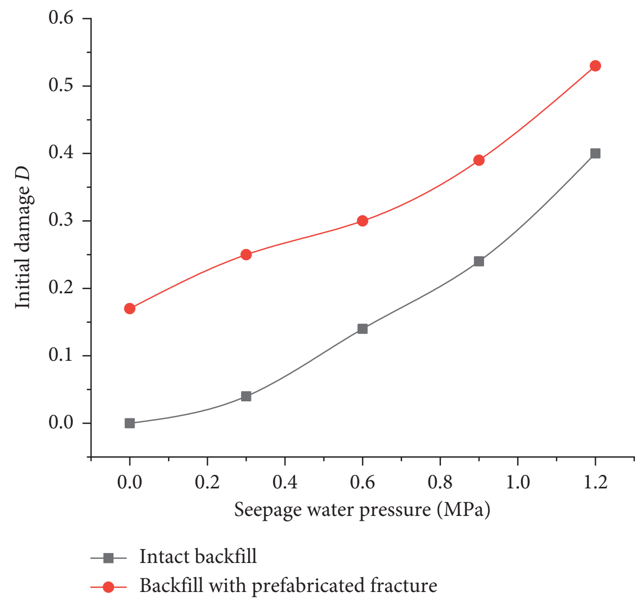

Figure 5: Relationship curves between initial damage and seepage water pressure.

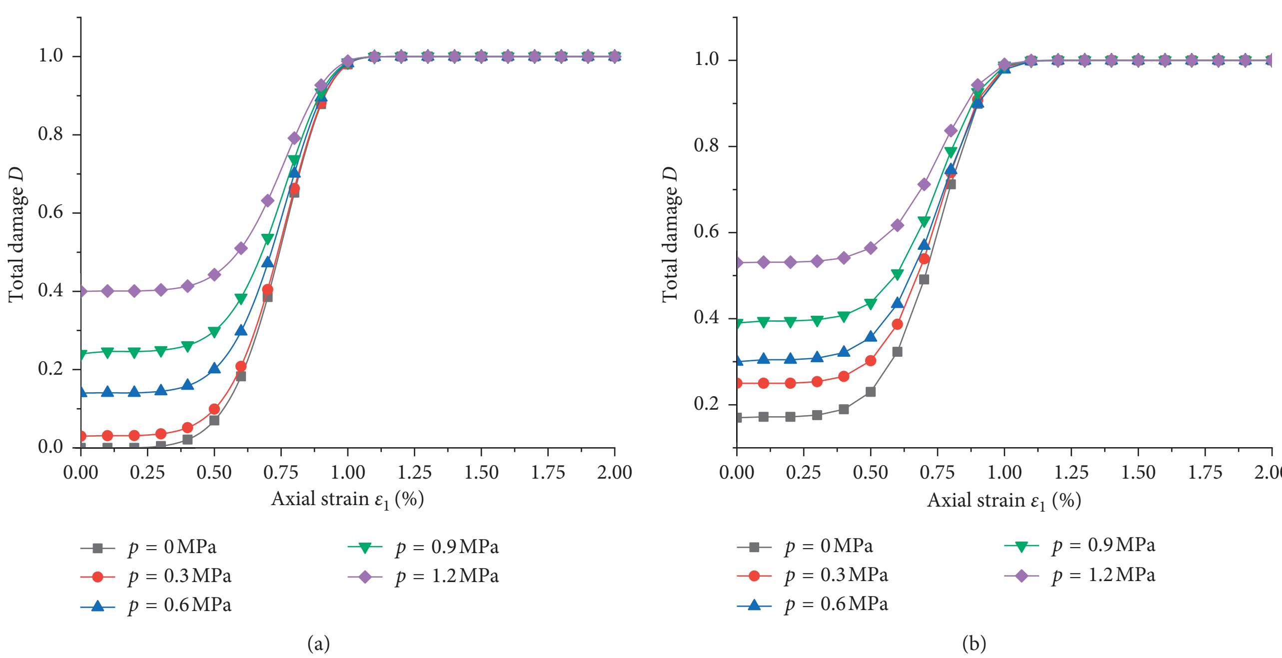

Figure 6: Damage evolution curves of backfill under different seepage water pressures. (a) Intact backfill. (b) Backfill with prefabricated fracture.

For the intact backfill, the total damage evolution law generally presents an S-shaped distribution with the increase of axial strain. At the initial stage of loading, the micropores and microfractures of the backfill are "compressed" to reduce the porosity and increase the density of the backfill, showing a compaction stage, and then the backfill is in a linear development stage. With the increase of axial strain, the micropores and microfractures in the backfill develop and evolve continuously, and the damage accelerates until the damage variable tends to 1. The whole process reflects the continuous generation and expansion of microfractures in the backfill from the microscopic point of view, and the deterioration of the mechanical properties of backfill from the macroscopic point of view. The development trend of damage evolution curves of backfill with prefabricated fracture is similar to that of intact backfill; that is, the existence of prefabricated fracture does not affect the development trend of damage evolution curves.

For the intact backfill, when the strain is 0, the initial damage of the backfill is the seepage mesodamage. For backfill with prefabricated fracture, when the strain is 0, the initial damage of backfill is the coupling damage of seepage and fracture. With the increase of seepage water pressure, the initial damage increases gradually, and the cumulative damage process is more significant. It shows that the inclined section of damage evolution curves is shortened, and the macroscopic performance is that the backfill reaches the failure faster and the residual strength is lower.

For the intact backfill, when the seepage water pressure increases from 0.0 MPa to 1.2 MPa, the initial seepage damage of the backfill increases from 0.0 to 0.40. The value of seepage damage is relatively small, indicating that the mechanical properties of the backfill are mainly affected by the load at this time, and its compressive capacity is strong, but with the increase of the seepage water pressure, its compressive capacity is gradually weakened. For backfill with prefabricated fracture, when the seepage water pressure is 1.2 MPa, the initial seepage damage is 0.53, which is relatively large, indicating that the mechanical properties of the backfill are mainly affected by the coupling effect of fracture and seepage and its compressive capacity is poor.

4.2. Influence of Confining Pressure on Backfill Damage. It can be seen from Figure 7 that the development trend of the damage evolution curves of the backfill under different confining pressure conditions is basically the same. With the increase of the axial strain, the damage evolution curves show an S-type development trend. The development trend of the curves is slightly different under different confining pressure conditions. For the same strain value, the larger the confining pressure is, the smaller the total damage of the backfill is.

As can be seen from Figure 7(a), the initial seepage damage of the backfill decreases with the increase of confining pressure and the damage accumulation process becomes slower. It shows that the inclined section of the damage evolution curves increases and the macroscopic performance shows that the backfill achieves slower damage and higher residual strength. For example, when the confining pressure increases from 0.5 MPa to 2.0 MPa, the initial seepage damage of the backfill decreases from 0.14 to 0.02 and the drop rate reaches 0.12, which is 85.7% lower. It shows that, with the increase of confining pressure, the damage and degradation effect of seepage on the strength of the backfill is weakened. This is because the high confining pressure suppresses the expansion of the fracture in the backfill and the internal fracture is tightly closed.

It can be seen from Figure 7(b) that, under the same confining pressure and seepage water pressure, the initial damage of the backfill with prefabricated fracture is greater than that of the intact backfill. Compared with the intact backfill, when the confining pressure increases from 0.5 MPa to 2.0 MPa, the initial damage of the backfill with prefabricated fracture increases by 0.32, 0.21, 0.13, and 0.08, respectively. It indicates that the prefabricated fracture deteriorates the strength of the backfill, but as the confining pressure increases, the damage of the prefabricated fracture to the strength of the backfill is weakened.

5. Discussion

We have shown that the damage evolution model of backfill established by the macrostatistical damage model, considering the coupling effect of seepage, stress, and initial fracture, is highly consistent with the test curve. Based on the damage evolution model and test data, the damage evolution characteristics of the backfill with prefabricated fracture under the seepage stress coupling were analyzed. We found that prefabricated fractures and seepage have significant effects on the damage of the backfill, and the total damage under the coupling is more serious than that under the single factor. By comparing the total damage evolution curves of backfill under different confining pressure conditions, we found that confining pressure has a certain inhibitory effect on the damage evolution of backfill, which is consistent with the conclusions of laboratory tests.

Liu et al. [29] revealed the three-dimensional damage and energy consumption law of backfill with different proportions according to the mechanical test of four kinds of cement tailing backfill with different proportions of lime sand; Zhao and Liu [30, 31] and other researchers established the damage constitutive model of backfill under uniaxial compression, based on the statistical damage theory. Zhang [32] established two different damage constitutive equations by studying the microdamage mechanism of backfill. The above literatures are based on the macrostatistical damage model, the damage evolution model of the backfill and the damage characteristics of the backfill under load are analyzed and studied. It is found that the damage evolution curve of the backfill is S-shaped as the axial strain increases, and it is consistent with the conclusion of this paper. However, the above literature does not consider the influence of seepage and prefabricated cracks on the damage of backfill. According to the research in this paper, it is found that prefabricated fractures and seepage have significant effects on the damage of the backfill, and the total damage under the coupling effect is more serious than that under the single factor. Therefore, it is of great theoretical and engineering significance to introduce seepage and cracks into the damage evolution model of the backfill.

The primary contribution of this paper is proposing the concepts of fracture macrodamage, loaded mesodamage, seepage mesodamage, and total damage of the backfill and establishing the damage evolution model of backfill with prefabricated fracture considering the coupling effect of seepage and stress. The damage constitutive equation is expected to promote mining development in the following aspects: (a) understanding the damage constitutive relationship and deformation characteristics of the backfill with prefabricated fracture; (b) providing an accurate constitutive model for the backfill with prefabricated fracture under the coupling of seepage and stress; (c) identifying potential risks by estimating the stability of backfill after filling mining in deep high-stress and high-seepage water pressure mine.

The omission of chemical factors is a clear limitation of the current study, because the chemical composition of underground water in coal mines is relatively

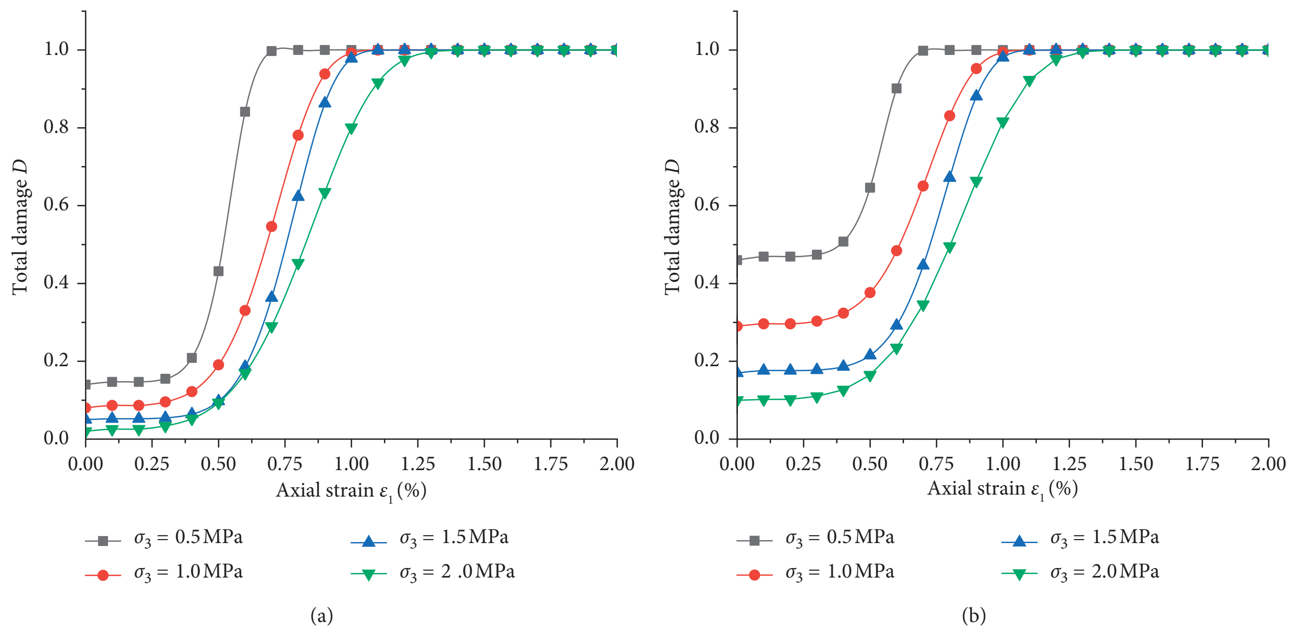

Figure 7: Damage evolution curves of backfill under different confining pressures. (a) Intact backfill. (b) Backfill with prefabricated fracture.

complex. Another limitation is that the number of tests is very small and only one kind mix proportion of backfill is studied.

6. Conclusions

(1) The concepts of fracture macrodamage, loaded mesodamage, seepage mesodamage, and total damage of backfill were proposed and the damage evolution model of backfill with prefabricated fracture considering the coupling effect of seepage and stress was established. The damage model established in this paper is in good agreement with the laboratory test results, can better reveal the damage evolution laws of the backfill with prefabricated fracture under seepage-stress coupling, and has certain rationality and feasibility.

(2) Fracture and seepage have significant effects on the damage and deterioration of the backfill. When the seepage water pressure is low, the fracture damage dominates; however, when the seepage water pressure is high, the seepage damage dominates; the total damage under the coupling action is more serious than the single factor.

(3) The development laws of the total damage evolution curves under different seepage water pressure and confining pressure are basically the same and the overall distribution is "S" type with the increase of axial strain. With the increase of confining pressure, the damage degradation effect of fracture and seepage on the strength of backfill is weakened and it indicates that confining pressure has a certain inhibition effect on the damage evolution of backfill.

Data Availability

All data are available within the article or can be obtained from the corresponding author upon request.

Conflicts of Interest

The authors declare that they have no conflicts of interest.

Acknowledgments

This work was supported by National Natural Science Foundation of China (Grant No. 51774195) and National Key Research and Development Program (2018YFC0604700).

References

[1] F. Cihangir, B. Ercikdi, A. Kesimal, A. Turan, and H. Deveci, "Utilisation of alkali-activated blast furnace slag in paste backfill of high-sulphide mill tailings: effect of binder type and dosage," *Minerals Engineering*, vol. 30, pp. 33–43, 2012.

[2] B. Cui, Y. Liu, H. Guo, Z. Liu, and Y. Lu, "Experimental study on the durability of fly ash-based filling paste in environments with different concentrations of sulfates," *Advances in Materials Science and Engineering*, vol. 2018, Article ID 4315345, 12 pages, 2018.

[3] C. C. Qi and A. Fourie, "Cemented paste backfill for mineral tailings management: review and future perspectives," *Minerals Engineering*, vol. 144, Article ID 106025, 2019.

[4] B. Ercikdi, F. Cihangir, A. Kesimal, and H. Deveci, "Practical importance of tailings for cemented paste backfill," *Paste Tailings Management*, pp. 7–32, 2017.

[5] S. Chen, D. Yin, F. Cao, Y. Liu, and K. Ren, "An overview of integrated surface subsidence-reducing technology in mining areas of China," *Natural Hazards*, vol. 81, no. 2, pp. 1129–1145, 2016.

[6] W. Zhu, J. Xu, J. Xu, D. Chen, and J. Shi, "Pier-column backfill mining technology for controlling surface subsidence," *International Journal of Rock Mechanics and Mining Sciences*, vol. 96, pp. 58–65, 2017.

[7] M. Li, J. X. Zhang, Y. L. Huang, and N. Zhou, "Effects of particle size of crushed gangue backfill materials on surface subsidence and its application under buildings," *Environmental Earth Sciences*, vol. 76, no. 17, pp. 603–620, 2017.

[8] Y. H. Yu and L. Q. Ma, "Application of roadway backfill mining in water-conservation coal mining: a case study in Northern Shaanxi, China," *Sustainability*, vol. 11, no. 13, pp. 1–22, 2019.

[9] M. Li, J. X. Zhang, X. X. Miao et al., "Strata movement under compaction of solid backfill," *Journal of China University of Mining and Technology*, vol. 43, no. 6, pp. 969–973, 2014.

[10] J. C. Wang and S. L. Yang, "Research on support-rock system in solid backfill mining methods," *Journal of China Coal Society*, vol. 35, no. 11, pp. 1821–1826, 2010.

[11] Q. D. Qu, L. Yao, X. H. Li et al., "Key factors affecting control surface subsidence in backfilling mining," *Journal of Mining & Safety Engineering*, vol. 27, no. 4, pp. 458–462, 2010.

[12] S. J. Chen, W. J. Guo, H. Zhou, and W. Guo-Hui, "Structure model and movement law of overburden during strip pillar mining backfill with cream-body," *Journal of China Coal Society*, vol. 36, no. 7, pp. 1081–1086, 2011.

[13] A. Fourie, M. Fahey, and M. Helinski, "Consolidation in accreting sediments: gibson's solution applied to backfilling of mine stopes," *Geotechnique*, vol. 60, no. 11, pp. 877–882, 2010.

[14] M. K. Mishra and U. M. R. Karanam, "Geotechnical characterization of fly ash composites for backfilling mine voids," *Geotechnical and Geological Engineering*, vol. 24, no. 6, pp. 1749–1765, 2006.

[15] W. B. Xu, C. B. Wan, and X. C. Tian, "Growth distribution laws and characterization methods of cracks of compact sandstone subjected to triaxial stress," *Journal of Mining & Safety Engineering*, vol. 35, no. 3, pp. 612–619, 2018.

[16] J. X. Fu, C. F. Du, and W. D. Song, "Strength sensitivity and failure mechanism of full tailings cemented backfills," *Journal of University of Science and Technology Beijing*, vol. 36, no. 9, pp. 1149–1157, 2014.

[17] C. H. Park and A. Bobet, "Crack coalescence in specimens with open and closed flaws: a comparison: a comparison," *International Journal of Rock Mechanics and Mining Sciences*, vol. 46, no. 5, pp. 819–829, 2009.

[18] Y. M. Yang, Y. Ju, L. T. Mao et al., "Growth distribution laws and characterization methods of cracks of compact sandstone subjected to triaxial stress," *Chinese Journal of Geotechnical Engineering*, vol. 36, no. 5, pp. 864–872, 2014.

[19] H. Hadi, K. Shahriar, M. F. Marji, and P. Moarefvand, "Cracks coalescence mechanism and cracks propagation paths in rock-like specimens containing pre-existing random cracks under compression," *Journal of Central South University*, vol. 21, no. 6, pp. 2404–2414, 2014.

[20] H. Hadi, A. Khaloo, and M. F. Marji, "Experimental and numerical analysis of Brazilian discs with multiple parallel cracks," *Arabian Journal of Geosciences*, vol. 8, no. 8, pp. 5897–5908, 2015.

[21] W. L. Heek and S. Jeon, "An experimental and numerical study of fracture coalescence in pre-cracked specimen under uniaxial compression," *International Journal of Solids and Structures*, vol. 48, no. 6, pp. 979–999, 2011.

[22] R. C. Liu, Y. J. Jiang, B. Li, L. yuan, and D. Yan, "Nonlinear seepage behaviors of fluid in fracture networks," *Rock and Soil Mechanics*, vol. 37, no. 10, pp. 2817–2824, 2016.

[23] M. M. Liu, S. H. Hu, Y. F. Chen et al., "An analytical model for nonlinear flow parameters of fractured rock masses based on high pressure packer tests," *Journal of Hydraulic Engineering*, vol. 47, no. 6, pp. 752–762, 2016.

[24] K. Wang, J. C. Sheng, H. C. Gao et al., "Study on seepage characteristics of rough fracture under the coupling action of stress seepage erosion," *Rock and Soil Mechanics*, vol. 41, no. 1, pp. 1–9, 2019.

[25] J. Lemaitre, *A Course on Damage Mechanics*, Springer-Verlag, Berlin, Germany, 1996.

[26] Q. S. Zhang, G. S. Yang, and J. X. Ren, "New study of damage variable and constitutive equation of rock," *Chinese Journal of Rock Mechanics and Engineering*, vol. 22, no. 1, pp. 30–34, 2003.

[27] H. M. Zhang and G. S. Yang, "Research on damage model of rock under coupling action of freeze-thaw and load," *Chinese Journal of Rock Mechanics and Engineering*, vol. 29, no. 3, pp. 471–476, 2010.

[28] L. M. Zhang, S. R. Lv, and H. Y. Liu, "A dynamic damage constitutive model of rock mass by comprehensively considering macroscopic and mesoscopic flaws," *Explosion and Shock Waves*, vol. 35, no. 3, pp. 428–436, 2015.

[29] Z. X. Liu, X. B. Li, G. Y. Zhao et al., "Three-dimensional energy dissipation laws and reasonable matches between backfill and rock mass," *Chinese Journal of Rock Mechanics and Engineering*, vol. 29, no. 2, pp. 344–348, 2010.

[30] S. G. Zhao, D. L. Su, W. R. Wu et al., "Study on damage model of backfill based on Weibull distribution under uniaxial compression," *China Mining Magazine*, vol. 26, no. 2, pp. 106–111, 2017.

[31] Z. X. Liu, Q. L. Liu, and W. G. Dang, "On softening-hardening intrinsically constitutive model for damage of tailings-cemented filling body," *Journal of Shandong University of Science and Technology (Natural Science)*, vol. 31, no. 2, pp. 36–41, 2012.

[32] F. W. Zhang, *Investigations on solidified characteristics and mechanism of slag cementitious materials in mine filling*, Ph.D. dissertation, Wuhan University, Wuhan, Hubei, China, 2009.